

OPEN ACCESS Article

# Halloysite Nanotubes as Nanofillers to Reinforce Glass Ionomer Cements

James A Holder<sup>1,2</sup>, Lisa M McNally<sup>3</sup> and Michele E Barbour<sup>1,4\*</sup><sup>1</sup> Bristol Dental School, University of Bristol, UK<sup>2</sup> Kemdent Ltd, Swindon, UK<sup>3</sup> Bristol Dental Hospital, University Hospitals Bristol, UK<sup>4</sup> Pertinax Pharma Ltd, Bristol, UK

\* Correspondence: m.e.barbour@bristol.ac.uk; Tel.: +44-117-3429573

Academic Editor: Professor Jurgen Geis-Gerstorfer

Received: 26 September 2019; Accepted: 06 November 2019; Published: 22 November 2019

**Abstract:** Glass ionomer cements (GICs) have many clinically favourable properties such as adhesion to tooth tissues and moisture tolerance, but have low strength compared with other direct dental restorative materials, and this limits their applications. Nanomaterials have shown promise in reinforcing biomaterials, including cements. The aim of this study was to explore whether the compressive strength of a GIC could be enhanced using halloysite nanotubes (HNTs), a naturally occurring hollow tubular material derived from clays. 1-15% by mass HNT was incorporated into GICs, coupled with adjustments to the powder:liquid ratio to account for the lubricating properties of HNTs. Compressive strength was measured, and the most promising formulation further investigated with respect to other mechanical and physical properties. 5% HNTs with 5:1 powder:liquid increased compressive strength by 34% with respect to unmodified GIC (187 and 140 MPa respectively;  $p=0.0004$ ). Hardness and wear resistance also increased by 11% ( $p=0.0006$ ) and 22% ( $p=0.0139$ ) respectively. Diametral tensile strength was unchanged ( $p=0.795$ ) and fluoride release from HNT-GICs was reduced by an average of 14% over 28 days. In conclusion, these nano-reinforced cement materials with improved mechanical properties could ultimately provide GICs for a wider range of uses in restorative dentistry.

**Keywords:** glass ionomer cements; nanomaterials; strength; halloysite; clay minerals; nanotubes; mechanical properties

## 1. Introduction

Glass ionomer cements (GICs) have a range of clinical uses, but one factor which limits their applications is their low strength in comparison with other restorative materials [1]. Nanoparticles and associated structures such as nanofibres and nanoplates present a promising approach to reinforcing materials. By incorporating these into a microstructured material it is possible to create an integrated, hierarchical micro- and nano- structured material which can yield improvements in strength, toughness and crack-resistance, such as is observed in many natural materials [2].

Halloysite nanotubes (HNTs) are naturally-occurring aluminosilicate mineral materials derived from clays. They have a high aspect ratio and a hollow core, and this structure has made them a target both for material reinforcement and for loading of drugs within the inner lumen [3–5], with the additional benefit that they are considerably cheaper than alternatives such as carbon nanotubes [6].

Within the specific context of dental materials, most research into the applications of HNTs has had as the primary focus the incorporation of a drug into the material by loading it into the hollow core of the halloysite, but changes in mechanical properties were also measured in several of these studies. For instance, while resin-based composites supplemented with 8% by weight HNTs showed

either no change or a deterioration in mechanical properties [7,8], lower concentrations (<5%) of HNTs were effective in improving mechanical properties [9]. Hardness of adhesive resins was increased by moderate concentrations of HNTs [10], and hardness of denture base resins was enhanced by modest (0.3%), but not greater (0.6-0.9%), incorporation of HNTs [11].

While there have been no reports to date of incorporation of HNTs into GICs, there have been attempts to incorporate another nanostructured clay material, montmorillonite, into this material. Montmorillonite is characterised by nanoscale sheets as opposed to tubes, and when functionalised using 12-amino-dodecanoic acid this material increased the compressive fracture strength, although not the wear resistance, of GICs [12,13], illustrating that in principle nanostructured fillers that are chemically compatible with a GIC can beneficially affect mechanical properties.

The aim of this project was to explore whether incorporating HNTs into a commercial GIC could improve its mechanical properties. The composition of the filler is important, and the fact that halloysite is, like the glass particles in a GIC, composed primarily of aluminosilicate material, forms the basis, alongside its physical form, of the selection of HNTs for this investigation. The interaction of the GIC glass with the polyacrylic acid matrix is a key factor in its setting and consequent properties, and the partial dissolution of the glass surface following by the crosslinking of the polyacrylic acid chains provides a seamless interface between the two. Interfacial interactions are known to be critical in natural nanomaterials, and poor or inadequate interfacial bonding can explain a number of failed attempts to create synthetic nanomaterials [2]. Thus one reason that HNTs were selected for this application was that it was anticipated that the mineral would interact with the acid in a similar way to the glass, bonding with the matrix rather than creating interfacial voids or weaknesses.

## 2. Materials and Methods

### 2.1 Characterisation of HNTs

HNTs of grade MF4 were provided by Durtec GmbH (Neubrandenburg, Germany) and are described by the supplier as consisting of 47.5% silica, 36.6% alumina and 13.9% water. HNTs were investigated using Fourier transform infrared spectroscopy (FTIR) using a Spectrum 100 (Perkin Elmer, MA, USA) over wavenumber range 400-4000  $\text{cm}^{-1}$  and X-ray diffraction (XRD) using a Bruker D8 Advanced Powder X-ray diffractometer (Bruker Corporation, MA, USA) with Cu  $K\alpha$  radiation ( $\lambda=1.54 \text{ \AA}$ ) at  $2\theta$  values 5-85 and a step size of  $0.1^\circ$ .

HNTs were assessed for acid lability by being immobilised on a carbon-coated adhesive disc and immersing one side into a pH 2 (0.1 M) HCl solution for 15 minutes. The pH of the HCl solution was ascertained using a pH probe model EC620131 connected to an Orion 3-star benchtop pH meter (Thermo Fischer Scientific, Massachusetts, USA). After immersion, the disc was rinsed using deionized water, dried at  $37 \pm 2^\circ\text{C}$  for 24 h, cleaned with compressed air, sputtered coated with gold and imaged using scanning electron microscopy (SEM) (Phenom Pro, Phenom World, Eindhoven, Netherlands).

### 2.2 Preparation of cement specimens

GICs were prepared using Diamond Carve™ (Kemdent, Purton, UK) as the base material. Diamond Carve is a conventional, hand-mixed powder-liquid GIC in which the powder comprises a fluoroaluminosilicate glass mixed with dry polyacrylic acid (PAA), tartaric acid and polyvinyl phosphonic acid and the liquid a PAA solution. The HNTs were substituted for the fluoroaluminosilicate glass component of the GIC powder. The glass and HNTs were mixed by first shaking vigorously by hand for 10 seconds in a sealed universal plastic container measuring 120 mm in length and 25 mm in diameter, then mixing on a tube roller (Cole-Parmer, Staffordshire, UK) at 33 rpm for 30 minutes. After this, 100 steel or glass balls (5 mm diameter, 51.9 g total mass) were added and this was transferred to a BMT-50-S-M tube and milled at 3000 rpm for 20 minutes using an Ultra-Turrax® tube drive (both IKA, Staufen im Breisgau, Germany). Substitutions of HNTs for glass were made at 0, 1, 2, 3, 5, 10 and 15% by mass with the manufacturer's recommended powder: liquid ratio of 4:1, and the effect of changing the powder: liquid ratio was investigated by selecting the most promising

doping of HNTs and varying the quantity of liquid giving ratios of 4.44:1, 5:1 and 5.7:1 (10, 20 and 30% reductions in liquid respectively). Powder and liquid were combined using a stainless-steel spatula on a glass surface and mixed for a maximum of 60 seconds before being placed in a mould of material and dimensions that varied according to the test to be performed. Mixed cements were prepared and stored at  $37 \pm 2^\circ\text{C}$  for  $23 \pm 1$  h in a humid environment (sealed container containing wet tissue paper) before further investigation. A cement prepared with components as supplied (without milling, adjusting powder:liquid ratio or adding HNTs) was used as a baseline material.

### 2.3 Measurement of cement compressive strength

GIC specimens were prepared using stainless steel cylindrical split moulds of  $4.0 \pm 0.2$  mm diameter and  $6.0 \pm 0.3$  mm height. The moulds were placed between two steel discs to give flat, planoparallel surfaces; the discs were lined with acetate sheets to prevent the cements sticking to the discs. N=40 specimens were used. 0% HNT was investigated both with and without milling to ascertain what effect if any the milling had on CS. Each sample diameter was measured three times providing an average reading, and specimens were tested for CS by compressing the flat surfaces using a universal testing machine (Instron, Buckinghamshire, UK) with a crosshead speed of 0.5 mm/min and a load cell of 10 kN. The load at failure was used to calculate CS.

### 2.4 Measurement of other cement properties: Diametral tensile strength (DTS), hardness and wear

For DTS measurements, GIC specimens (n=40) were prepared using stainless steel cylindrical moulds of  $6.0 \pm 0.3$  mm diameter and  $4.0 \pm 0.2$  mm height. The moulds were placed between two steel discs to give flat, planoparallel surfaces; the discs were lined with acetate sheets to prevent the cements sticking to the discs. Each sample diameter was measured three times providing an average reading, and specimens were tested for DTS by compressing the curved edges using a universal testing machine (Instron, Buckinghamshire, UK) with a crosshead speed of 0.5 mm/min and a load cell of 10 kN. The load at failure was used to calculate DTS.

For hardness measurements, GIC specimens measuring  $6.0 \times 8.0 \times 3.2 (\pm 0.1)$  mm were prepared in silicone moulds and compressed between two 1 kg weights lined with acetate sheets to prevent sticking to the weights. The cement specimens were immobilised using stainless steel grips and tested for microhardness using Duramin 1 indenter fitted with a Vickers diamond tip (Struers, Rotherham, UK). A force of 1.961 N was applied to the cement for 20 seconds and indentation measurements were made using a  $\times 40$  lens CCD camera (Toshiba-Teli Co., Tokyo, Japan) by measuring the cross-sectional lengths of the indentations. Two samples of each cement were made on three different days (6 samples of each group) and 10 indentation measurements were made on each, five on each side of the cement. Any indents made on a pore or surface imperfection on the cements were rejected and the test repeated.

For wear measurements, GIC specimens measuring  $6.0 \times 8.0 \times 3.2 (\pm 0.1)$  mm were prepared in a silicone mould and compressed between two 1 kg weights lined with acetate sheets. One half of each specimen was covered using adhesive polyvinyl chloride (PVC) tape. Specimens were immersed in 500 mL of 19.1 mM citric acid adjusted using KOH to pH 3.3 in a rectangular bath. Specimens were brushed while immersed in this acid using a purpose-made tooth brushing machine which comprised a linear motion arm which held Colgate® medium extra clean toothbrush heads (Colgate Palmolive, New York, USA) affixed using sticky wax (Kemdent, Purton, UK) for 10000 brush cycles under a 200 g weight. After brushing the specimens were immersed in deionized water for 30 s, the PVC tape was removed and the specimens were imaged using a Scantron Proscan 2000 non-contact profilometer (Scantron Industrial Products Ltd., Taunton, UK). Any specimens where the PVC tape was dislodged during brushing were discarded.

### 2.5 Fluoride release from cements

GIC specimens were prepared using stainless steel cylindrical moulds of  $6.0 \pm 0.3$  mm diameter and  $4.0 \pm 0.2$  mm height giving a surface area of 132 mm<sup>2</sup>. Specimens were immersed in 20 mL DIW at  $37 \pm 2^\circ\text{C}$ . The DIW was refreshed at 1, 2, 3, 7, 14, 21 and 28 days and the water retained for fluoride

analysis. Fluoride-containing solutions were analysed using an Orion 96-09 ionplus® fluoride selective electrode (FSE) with an Orion 4 Star pH/ISE benchtop digital unit. The FSE was calibrated using standard fluoride solutions of 1000, 100, 10, 1 and 0.1 ppm. Solutions were mixed with Orion ionplus® Total Ionic Strength Adjustment Buffer (TISAB) II containing 1,2-cyclohexane diaminetetraacetic acid (CDTA) in a 1:1 ratio (all Thermo Fisher Scientific, Massachusetts, USA). All solutions were stored, measured and analysed in plastic containers.

### 2.6 Statistical analysis

Data sets were analysed using a one-way ANOVA and, where statistically significant differences were indicated ( $p < 0.05$ ), a Tukey HSD test. Data consisting of two groups only were analysed using a student t-test also using a significance level of 0.05.

## 3. Results

### 3.1 Characterisation of HNTs

An FTIR spectrum of HNTs is shown in Figure 1. Peaks were observed in the region of 551, 908, 1070 and 3640  $\text{cm}^{-1}$  which are comparable to published spectra of HNT [14]. An XRD spectrum of HNTs is shown in Figure 2. The peaks at  $2\theta=12, 20$  and  $24.9^\circ$  are comparable to published values [15].

SEM images of HNTs as received and after immersion in 0.1 M HCl for 15 minutes are shown in Figure 3. HNTs are visible as large aggregates with diameters up to 100  $\mu\text{m}$ . There was no indication that the HNTs were acid-labile under these conditions.

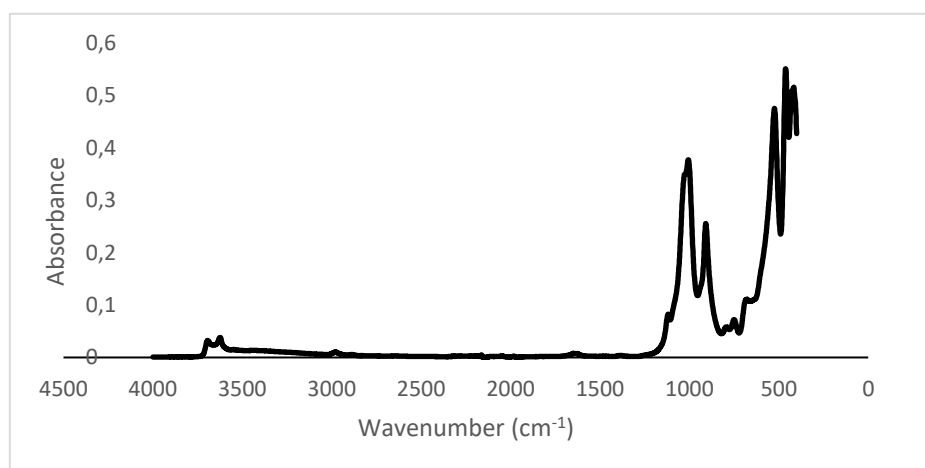


**Figure 1.** FTIR spectrum of HNTs. There are peaks in the regions of 520, 910, 1000 and 3640  $\text{cm}^{-1}$ , which are comparable to literature values for halloysite [14].

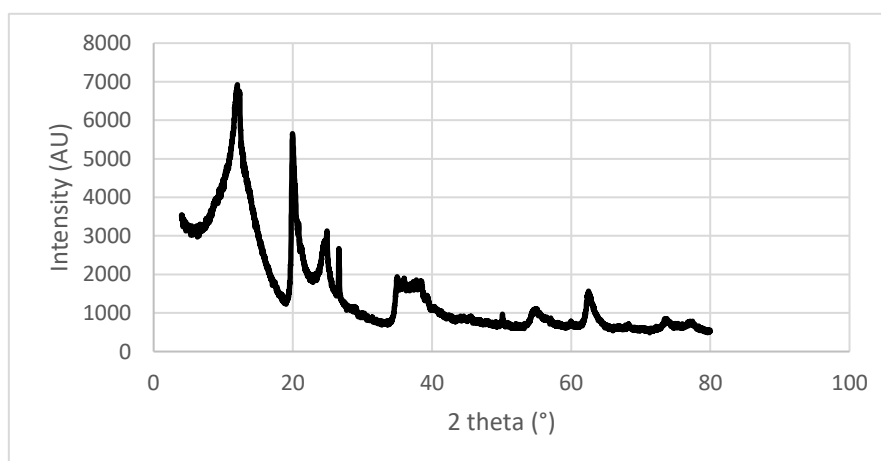


**Figure 2.** XRD spectrum of HNTs. The peaks at  $2\theta=12, 20$  and  $24.9^\circ$  are comparable to literature values [15].

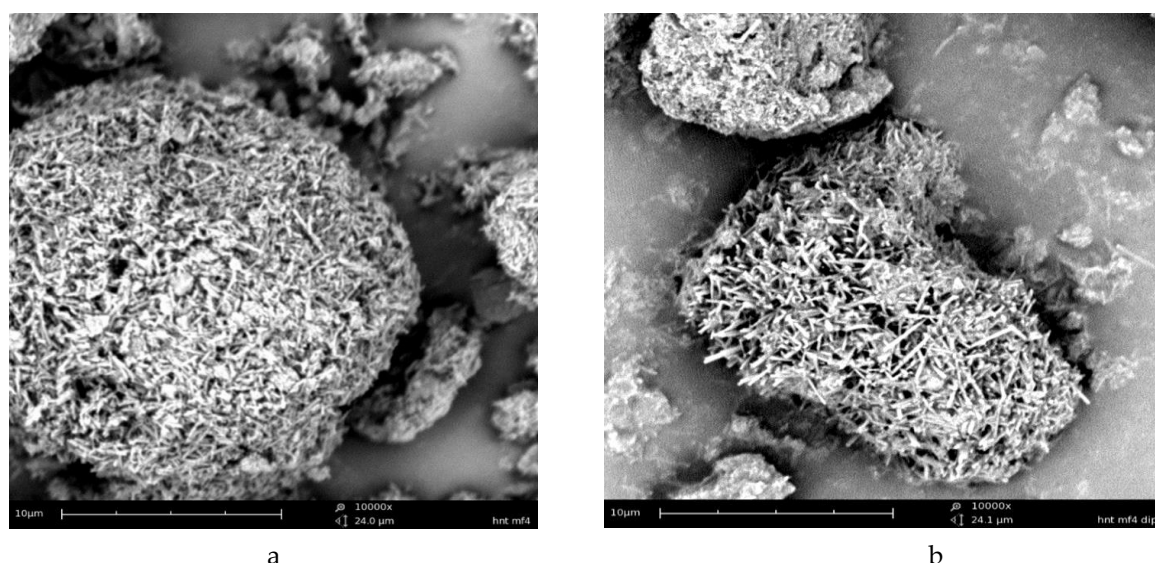


**Figure 3.** HNTs before (a) and after (b) immersion in pH 2 HCl for 15 minutes. Scale bars represent 10 μm.

### 3.2 Cement compressive strength

CS of specimens as a function of HNT doping is shown in Table 1. Only 5% HNT resulted in a small (12%) but statistically significant ( $p = 0.001$ ) increase in CS with respect to the unmodified GIC; all other dopings resulted in a CS that was equal to or lower than the original material. CS of specimens with 5% HNT by mass and varied powder: liquid ratio are shown in Table 2. A higher ratio (less liquid) gave an increase in strength. The greatest strength increase (34% greater than the unmodified GIC and 25% greater than the milled but otherwise unmodified GIC,  $p < 0.001$  for both cases) was 5% HNT with a powder: liquid ratio of 5:1 (20% less liquid than the manufacturer’s instructions specify) and this was therefore taken forward for further testing and comparison with the unmodified control. This cement is referred to as 5%-HNT-GIC as shorthand. It was not possible to prepare a comparator group with no HNT and a powder: liquid ratio of 5:1 as the mix was too dry and resulted in a crumbly, very friable cement. Therefore for all subsequently reported measurements, 5%-HNT-GIC was compared with Diamond Carve that had been milled but otherwise unmodified with a powder:liquid ratio of 4:1. This is referred to as control-GIC.

**Table 1.** Compressive strength of GIC specimens as a function of the % by mass HNT substituted for glass powder. Standard deviations are shown in parentheses. N=40 specimens were tested per group. Superscript letters represent statistically homogeneous groups.

% substitution of HNT for glass powder	Milled	Compressive strength [MPa] (SD)
0	No	140.2 (26.1) <sup>c</sup>
0	Yes	149.8 (21.2) <sup>c,d,e</sup>
1	Yes	122.3 (21.9) <sup>a,b</sup>
2	Yes	120.6 (15.2) <sup>a,b</sup>
3	Yes	118.8 (14.7) <sup>a</sup>
5	Yes	157.3 (23.2) <sup>d,e,f</sup>
10	Yes	145.1 (20.0) <sup>c,d</sup>

**Table 2.** Compressive strength of GIC specimens containing 5% HNT substituted by mass for glass powder, as a function of the powder:liquid ratio. Standard deviations are shown in parentheses. N=40 specimens were investigated per group. Superscript letters represent statistically homogeneous groups.

Powder: liquid ratio	Compressive strength [MPa] (SD)
4:1	157.3 (23.2) <sup>d,e,f</sup>
4.4:1	165.2 (16.5) <sup>e,f</sup>
5:1	188.0 (29.0) <sup>f,g</sup>
5.7:1	172.2 (29.9) <sup>f,g</sup>

### 3.3 Diametral tensile strength (DTS), hardness and wear

DTS, hardness and wear of 5%-HNT-GIC and control-GIC are shown in Table 3. DTS was not statistically significantly different between the two groups ( $p = 0.795$ ), whereas hardness increased with the addition of HNTs (57.7 compared with 52.2 VHN,  $p = 0.0006$ ) and wear resistance increased with the addition of HNTs (21.6  $\mu\text{m}$  compared with 27.8  $\mu\text{m}$  wear,  $p = 0.0139$ ).

**Table 3.** DTS, hardness and wear of control-GIC (milled, no HNT, standard 4:1 powder:liquid ratio) and 5%-HNT-GIC (milled, with 5% HNT and a powder: liquid ratio of 5:1). Standard deviations are shown in parentheses. The DTS were not statistically significantly different ( $p=0.795$ ) whereas statistically significant increases were observed in hardness ( $p = 0.0006$ ) and wear resistance ( $p=0.014$ ).

Parameter [unit]	Control GIC (SD)	5%-HNT-GIC (SD)
Diametral tensile strength [MPa]	6.7 (1.6)	6.8 (2.1)
Hardness [Vickers hardness number]	52.2 (7.9)	57.7 (6.2)
Wear after 10000 cycles of toothbrush abrasion in citric acid [ $\mu\text{m}$ ]	27.8 (3.2)	21.6 (5.8)

### 3.4 Fluoride release from cements

Fluoride release from control-GIC and 5%-HNT-GIC cements as a function of time are shown in Figure 4.

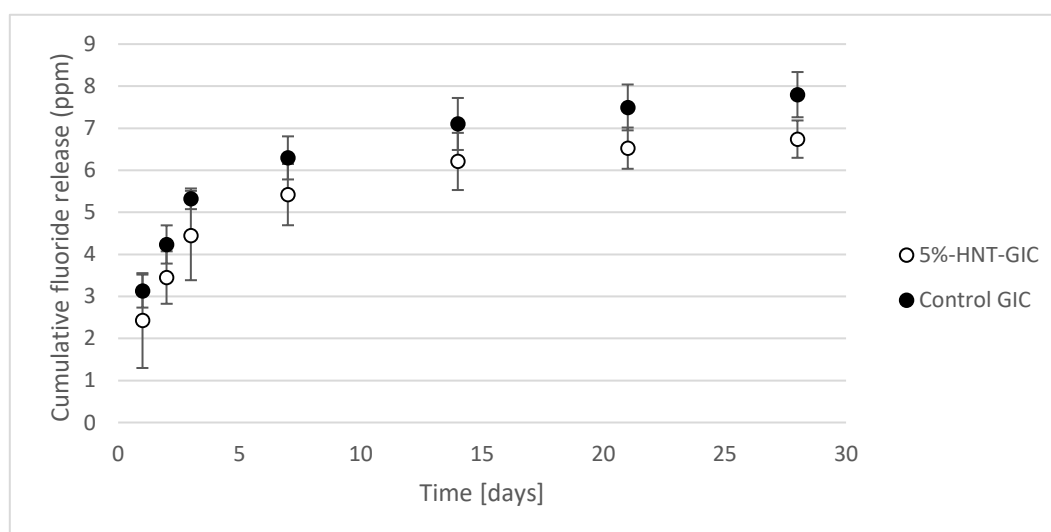


**Figure 4.** Cumulative fluoride release from control GIC (milled, no HNT, standard 4:1 powder:liquid ratio) and 5%-HNT-GIC (GIC, milled, with 5% HNT and a powder:liquid ratio of 5:1). Error bars represent standard error. Significant reductions in fluoride release were seen at days 1 ( $p = 0.0013$ ), 2 ( $p = 0.039$ ), 21 ( $p=0.0003$ ) and 28 ( $p = 2.23 \times 10^{-5}$ ).

There was a lower fluoride release from 5%-HNT-GIC compared with control-GIC; on average over the sample time this was 14% lower and was statistically significant at time points 24 h ( $p = 0.0013$ ), 48 h ( $p = 0.039$ ), 21 days ( $p = 0.0003$ ) and 28 days ( $p = 2.23 \times 10^{-5}$ ).

#### 4. Discussion

HNTs have been incorporated into other dental materials, for instance into resin-based composites and acrylics, with some observation of an enhancement of mechanical properties, although this was dose-dependent and not always unequivocal [7-11]. HNTs have not previously been incorporated into GICs. It was observed that the process of incorporating HNTs into the GIC components, by substituting for glass particles and ball milling, adversely affected the handling properties, yielding a wet, sloppy material that was difficult to mix and pack effectively. The milling process is important, as it is widely reported that poor dispersion of nanoparticles and related nanostructures in composite materials undermines the reinforcing process and gives disappointing results [16], and therefore it was not deemed appropriate to dispense with the milling step.

The observation that adding HNTs to the GIC made the mix less viscous is at first glance counterintuitive, in that the HNTs have a higher specific surface area than the GIC powder and thus one might expect that more liquid would be required to effectively wet the combined powder, rather than less. This observation is attributed to the lubricating properties of some nanoparticles, in that they can help the larger particles slide past one another and pack more readily and efficiently. This has been reported specifically for HNTs [17,18]. The regular tube-like structures of the HNTs in combination with the irregular and jagged glass particles create a blend that overall will move more freely past one another than the glass particles alone.

For this reason, a reduction in the GIC liquid component was explored, using the HNT doping that gave the highest strength without this modification, an albeit statistically insignificant increase of 5%. The optimum powder:liquid ratio was identified to be 5:1, as compared to the manufacturers' recommendation for the unmodified cement of 4:1. This, combined with a 5% HNT doping and milling, resulted in a CS of 187.2 MPa, 25% greater than the milled cement with a powder:liquid ratio of 4:1 (149.8 MPa) and 34% greater than the as-received unmilled cement (140.2 MPa). The proposed mechanism is one of reinforcement by the rod-like HNT structures; similar shaped nanotubes, rods and fibres have been used to enhance strength and related properties of a diverse range of materials including bioactive ceramics [19] and glasses [20], poly(methyl) methacrylate denture base resins [21], and hydrogel composites [22]. The mechanism of reinforcement is thought to be the creation of a multiscale interlocking system of the smaller nanotubes and the larger irregular glass particles, with the HNTs acting as an additional stress-bearing component, and resisting or deflecting crack propagation.

HNT were selected owing to their shape and size, their inexpensive, widely available nature, but also their chemical similarity to the glass used in a GIC. It was considered that they would withstand the acidic environment during the setting of the GIC, unlike some other material such as calcium phosphates which degrade rapidly under acidic conditions. The observation that the HNTs withstood 15 minutes immersion in pH 2 acid supports this hypothesis, although the lack of increase in tensile strength does imply that any interaction of this kind was insufficient to render the material stronger under tensile load.

The aspiration to increase the strength of a GIC is not a new one. While resin-modified GICs have many favourable properties including good mechanical performance, the incorporation of the resin brings the requirement for a more time consuming and meticulous application procedure. Approaches to enhancing strength without resins include the use of metals, glass fibres, zirconia, as well as various nanoparticles, and have been reviewed recently [23]. Titanium dioxide nanoparticles increased compressive strength of a GIC by 18% [24], which was attributed to the packing of the nanoparticles between the much larger glass particles. These titanium dioxide nanoparticles were roughly spherical, whereas other studies have suggested that high aspect ratio particles such as the HNTs used here might offer additional benefits over simply filling in the spaces between the glass particles. Glass fibres, much larger than the HNTs used here (10  $\mu\text{m}$  diameter), were found to

improve a number of mechanical properties of a GIC including tensile strength, hardness and flexural strength [25].

The increase in surface hardness with the incorporation of HNTs has been observed in other materials [26,27]. It has been reported that if HNTs are not well distributed through the material hardness can decrease, and the increase observed here may thus be taken as an indication that the milling process was at least moderately successful in distributing the HNTs through the GIC matrix.

Wear testing using tooth brushing simulations has been used for some decades to assess relative wear resistance of tooth tissues and restorative materials [28]. As citric acid is well established to erode dental tissues, this was used to provide a greater challenge to the acid labile GICs. The reduction in wear observed with the 5%-HNT-GICs suggests that the reinforcing properties of the HNTs also provide some degree of protection, likely by the same mechanism by which the HNTs increase strength, in addition to the fact that the HNTs are inherently less acid soluble than the base GIC.

The 5%-HNT-GIC released less fluoride than the control GIC, on average by 14%. This can only partially be attributed to the reduced glass content owing to the substitution of HNTs for the glass; there is 5% less fluoride in the 5%-HNT-GICs than the control GICs. The reduced PAA liquid content may also have contributed as the carboxylic acid is responsible for releasing the fluoride during the setting reaction. The fluoride ions are released codependently alongside counter-cations of sodium and calcium and are therefore dependent on these. Of course whether the reduced fluoride release has any clinical implication is unclear as there is no consensus on whether there is a threshold fluoride release to elicit a favourable response, and if so, what this threshold is.

In conclusion, the substitution of HNTs for 5% of the fluoroaluminosilicate component in a conventional GIC with milling led to a 34% increase in CS, 9.5% increase in hardness and reduced wear by 22.3%. Tensile strength was not affected, and fluoride release was slightly reduced. These novel nano-reinforced cements may, with further development and validation, prove useful in expanding the range of applications for GICs.

**Acknowledgments:** The research described herein was supported by a PhD studentship for JA Holder from Kemdent Ltd and by the University of Bristol.

**Author Contributions:** Holder, McNally and Barbour conceived and designed the experiments, Holder conducted the experiments, Holder and Barbour analysed the data and wrote the paper and McNally reviewed the paper.

**Conflicts of Interest:** The research presented here was conducted as part of the PhD research of JA Holder. Dr Holder was at the time of conducting the research described herein both a PhD student and an employee of Kemdent Ltd who provided sponsorship and some of the materials for their PhD. The sponsors had no role in the design of the study, in the collection, analysis, or interpretation of data, or in the writing of the manuscript. Drs LM McNally and ME Barbour have no conflicts of interest to declare.

## References

1. Sidhu, S.K. Glass-ionomer cement restorative materials: a sticky subject? *Aust Dent J* 2011, 56, 23–30. DOI 10.1111/j.1834-7819.2010.01293.x.
2. Peng, J.; Cheng, Q. High-Performance Nanocomposites Inspired by Nature. *Adv Mater.* 2017, 29, 1–16. DOI 10.1002/adma.201702959.
3. Ji, L.; Qiao, W.; Zhang, Y.; Wu, H.; Miao, S.; Cheng, Z.; et al. A gelatin composite scaffold strengthened by drug-loaded halloysite nanotubes. *Mater Sci Eng C* 2017, 78, 362–9. DOI 10.1016/j.msec.2017.04.070.
4. Liu, M.; Dai, L.; Shi, H.; Xiong, S.; Zhou, C. In vitro evaluation of alginate/halloysite nanotube composite scaffolds for tissue engineering. *Mater Sci Eng C* 2015, 49, 700–12. DOI 10.1016/j.msec.2015.01.037.



5. Jing, X.; Mi, H.Y.; Turng, L.S. Comparison between PCL/hydroxyapatite (HA) and PCL/halloysite nanotube (HNT) composite scaffolds prepared by co-extrusion and gas foaming. *Mater Sci Eng C* 2017, *72*, 53–61. DOI 10.1016/j.msec.2016.11.049.
6. Yuan, P.; Tan, D.; Annabi-Bergaya, F. Properties and applications of halloysite nanotubes: Recent research advances and future prospects. *Appl Clay Sci* 2015, *112–113*, 75–93. DOI 10.1016/j.clay.2015.05.001
7. Degrazia, F.W.; Leitune, V.C.B.; Takimi, A.S.; Collares, F.M.; Sauro, S. Physicochemical and bioactive properties of innovative resin-based materials containing functional halloysite-nanotubes fillers. *Dent Mater* 2016, *32*, 1133–43. DOI 10.1016/j.dental.2016.06.012
8. Cunha, D.A.; Rodrigues, N.S.; Souza, L.C.; Lomonaco, D.; Rodrigues, F.P.; Degrazia, F.W.; et al. Physicochemical and microbiological assessment of an experimental composite doped with triclosan-loaded halloysite nanotubes. *Materials* 2018, *11*, 1080. DOI 10.3390/ma11071080.
9. Chen, Q.; Zhao, Y.; Wu, W.; Xu, T.; Fong, H. Fabrication and evaluation of Bis-GMA/TEGDMA dental resins/composites containing halloysite nanotubes. *Dent Mater* 2012, *28*, 1071–9. DOI 10.1016/j.dental.2012.06.007.
10. Feitosa, S.A.; Münchow, E.A.; Al-Zain, A.O.; Kamocki, K.; Platt, J.A.; Bottino, M.C. Synthesis and characterization of novel halloysite-incorporated adhesive resins. *J Dent* 2015, *43*, 1316–22. DOI 10.1016/j.jdent.2015.08.014.
11. Abdallah, R.M. Evaluation of polymethyl methacrylate resin mechanical properties with incorporated halloysite nanotubes. *J Adv Prosthodont* 2016, *8*, 167–71. DOI 10.4047/jap.2016.8.3.167.
12. Dowling, A.H.; Stamboulis, A.; Fleming, G.J.P. The influence of montmorillonite clay reinforcement on the performance of a glass ionomer restorative. *J Dent* 2006, *34*, 802–10. DOI 10.1016/j.jdent.2006.03.005.
13. Dowling, A.H.; Fleming, G.J.P. The impact of montmorillonite clay addition on the in vitro wear resistance of a glass-ionomer restorative. *J Dent* 2007, *35*, 309–17. DOI 10.1016/j.jdent.2011.12.002
14. Bediako, E.G.; Nyankson, E.; Dodoo-Arhin, D.; Agyei-Tuffour, B.; Łukowiec, D.; Tomiczek, B.; et al. Modified halloysite nanoclay as a vehicle for sustained drug delivery. *Heliyon*. 2018, *4*, e00689. DOI 10.1016/j.heliyon.2018.e00689.
15. Dong, Y.; Marshall, J.; Haroosh, H.J.; Mohammadzadehmoghadam, S.; Liu, D.; Qi, X.; et al. Polylactic acid (PLA)/halloysite nanotube (HNT) composite mats: Influence of HNT content and modification. *Compos Part A Appl Sci Manuf* 2015, *76*, 28–36. DOI 10.1016/j.compositesa.2015.05.011.
16. Liu, M.; Jia, Z.; Jia, D.; Zhou, C. Recent advance in research on halloysite nanotubes-polymer nanocomposite. *Prog Polym Sci* 2014, *39*, 1498–525. DOI 10.1016/j.progpolymsci.2014.04.004/
17. Sahnoune, M.; Kaci, M.; Taguet, A.; Delbé, K.; Mouffok, S.; Abdi, S.; et al. Tribological and mechanical properties of polyamide-11/halloysite nanotube nanocomposites. *J Polym Eng* 2018, *39*. DOI 10.1515/polyeng-2018-0131.
18. Bernal, J.P.; Parás, L.P.; Ramirez, R.T. Tribological properties study of lubricants for possible nanoclays reinforced biomedical applications. VII Lat Am Congr Biomed Eng CLAIB 2016, Bucaramanga, Santander, Colomb Oct 26th -28th, 2016, *60*, 341–2. DOI 10.1007/978-981-10-4086-3
19. Gao, C.; Feng, P.; Peng, S.; Shuai, C. Carbon nanotube, graphene and boron nitride nanotube reinforced bioactive ceramics for bone repair. *Acta Biomater* 2017, *61*, 1–20. DOI 10.1016/j.actbio.2017.05.020
20. Dixit, K.; Sinha, N. Compressive Strength Enhancement of Carbon Nanotube Reinforced 13-93B1 Bioactive Glass Scaffolds. *J Nanosci Nanotechnol* 2019, *19*, 2738–46. DOI 10.1166/jnn.2019.16029
21. Somkuwar, S.; Mishra, S.; Agrawal, B.; Choure, R. Comparison of the flexural strength of polymethyl methacrylate resin reinforced with multiwalled carbon nanotubes and processed by conventional water bath technique and microwave polymerization. *J Indian Prosthodont Soc* 2017, *17*, 332–9. DOI 10.4103/jips.jips\_137\_17.
22. Huang, B.; Liu, M.; Zhou, C. Chitosan Composite Hydrogels Reinforced with Natural Clay Nanotubes. *Carbohydr Polym* 2017, *175*, 689–98. DOI 10.1016/j.carbpol.2017.08.039.
23. Ching, H.S.; Luddin, N.; Kannan, T.P.; Ab Rahman, I.; Abdul Ghani, N.R.N. Modification of glass ionomer cements on their physical-mechanical and antimicrobial properties. *J Esthet Restor Dent*. 2018, *30*, 557–551. DOI 10.1111/jerd.12413.
24. Elsaka, S.E.; Hamouda, I.M.; Swain, M.V. Titanium dioxide nanoparticles addition to a conventional glass-ionomer restorative: Influence on physical and antibacterial properties. *J Dent* 2011, *39*, 589–98. DOI 10.1016/j.jdent.2011.05.006.

25. Hamouda, I. Reinforcement of conventional glass-ionomer restorative material with short glass fibers. *J Mech Behav Biomed Mater* 2009, 2, 73–81. DOI 10.1016/j.jmbbm.2008.04.002.
26. Du, M.; Guo, B.; Lei, Y.; Liu, M.; Jia, D. Carboxylated butadiene-styrene rubber/halloysite nanotube nanocomposites: Interfacial interaction and performance. *Polymer* 2008, 49, 4871–6. DOI 10.1016/j.polymer.2008.08.042.
27. Albdiry, M.T.; Yousif, B.F. Morphological structures and tribological performance of unsaturated polyester based untreated/silane-treated halloysite nanotubes. *Mater Des* 2013, 48, 68–76. DOI 10.1016/j.matdes.2012.08.035.
28. Absi, E.G.; Addy, M.; Adams, D. Dentine hypersensitivity – the effect of toothbrushing and dietary compounds on dentine in vitro: an SEM study. *J Oral Rehabil* 1992, 19, 101–10. DOI 10.1111/j.1365-2842.1992.tb01086.x.



© 2019 by the authors. Submitted for possible open access publication under the terms and conditions of the Creative Commons Attribution (CC-BY) license (<http://creativecommons.org/licenses/by/4.0/>).